Surface and line-edge roughness in solution and plasma developed negative tone resists: Experiment and simulation

G. P. Patsis, A. Tserepi, I. Raptis, N. Glezos, and E. Gogolides[a)]
Institute of Microelectronics, NCSR ''Demokritos,'' 15310 Aghia Paraskevi, Greece

E. S. Valamontes
Technological Educational Institute of Athens, Aegaleo 12210, Greece

(Received 1 June 2000; accepted 24 August 2000)

A methodology is described for the experimental and theoretical study of surface roughness (SR) and line-edge roughness (LER) and their relation for solution and plasma developed resist schemes. Experimental results for a negative-tone nonchemically amplified siloxane bilayer resist scheme are shown. In addition, a molecular-type simulation of SR and LER is presented. The simulator can follow the appearance of SR and LER after each process step and predict the roughness dependence on material properties and process conditions. The simulation results are compared with SR experimental data for a negative-tone chemically amplified epoxy resist. © *2000 American Vacuum Society.* [S0734-211X(00)12406-0]

I. FRAMEWORK FOR SR AND LER STUDIES

The lithographic processes for this decade are facing the demands of the sub-100 nm range of characteristic dimension. For such small dimensions, the roughness of lithographic materials/processes places a significant limitation on the quality of the printed lines and the critical dimension (CD) control. It is suspected that even the size of polymer chains and the conformation of a single segment of a chain can affect roughness. Because of its importance in the last few years, several publications discuss the problem of roughness.[1–9]

Surface roughness (SR) appears after the spin coating of the photoresist film, while line edge roughness (LER) appears after the development of the microstructure. However, the two phenomena are closely related. Figure 1 shows a schematic of the origins of SR and LER. They are material and process dependent. The final roughness is a convolution of the roughness induced by each process step. The photoresist film has a SR characteristic of the resist material. The exposure and postexposure bake of the film induce chemical changes, such as deprotection or crosslinking. These changes induce an increase or at least a change of the SR of the photoresist. Upon total or partial development, these changes are magnified and are observed as different SR as a function of dose. Thus, each processing step may induce an increase or at least a change in the SR of the resist. Such steps include solution development, or plasma development, and the subsequent etching steps for the antireflective coating and the substrate.

LER appears after solution or plasma development. If the latent image were ideal (e.g., a square wave modulation with values 0 and 1), then the difference between SR and LER would be that the former reflects the resist/air interface, while the latter reflects the exposed/unexposed resist interface, which becomes a resist/air interface after development. Thus, at least for the solution development process (isotropic process) the LER has the same origin as the SR[1] with mainly one additional element: It depends on the details of the latent image induced by the exposure system. However, for plasma developed photoresists, and for the subsequent etching steps (anisotropic processes), SR and LER may differ in origin. Any investigation should include measurements and simulation of the whole spectrum of materials and processes shown in Fig. 1. In addition, questions related to the measurements needed to characterize roughness, such as rms measurements from atomic force microscopy (AFM), fractal dimensions, scanning electron microscope (SEM) measurements, etc.[1,7] should be addressed.

Within the framework described above, our work includes both the experimental study of SR and LER (for solution and also plasma developed resists), and roughness simulations, as well as investigation of the relation between SR and LER. In the limited space of this article we will present our first experimental results from a class of bilayer resists, and our first results from a SR and LER simulator, which will be compared to SR data for a negative-tone solution developed chemically amplified resist (CAR).

Sometimes it is thought that plasma developed resists suffer from high (or at least higher) LER compared to solution developed systems. However, Si-containing polymers show great promise as prospective materials for lithography at 157 nm and below, provided that they exhibit good resolution and CD control appropriate for nanopatterning. To shed some light on the issue of roughness in silicon containing systems, we evaluate siloxanes in this work as materials for bilayer lithographic schemes, based on measurements of SR and LER as a function of exposure dose and plasma development conditions. Siloxanes are not aqueous-base developed resists, and thus will not be used for 157 nm lithography. However, they are used here as simple model resists of

[a)]Electronic mail: evgog@imel.demokritos.gr

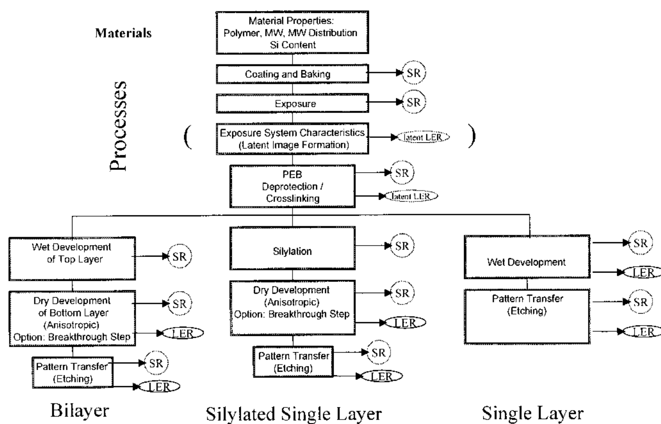

FIG. 1. Schematic of the origins of SR and LER for three lithographic schemes.

known properties and chemistry, based also on the experience existing in our group headed by Hatzakis.[10] 157 nm resists could contain siloxane copolymers making this study quite relevant. This work will be described in Sec. II.

A careful look at Fig. 1 also reveals that simulation of material, exposure, and other process related roughness is a huge task. In this work we take the first step to address the simulation problem. First of all, the exposure system characteristics, which are extremely important for LER, will be ignored, despite our suspicion that they might be the most important cause of LER. Although our simulator can easily accept as input the latent image of an electron beam or an optical lithography simulator, we chose not to do this at this stage: Instead, an ideal square wave-type exposure was considered. We thus assumed that the transfer function of the exposure system is unity, and tried to see what the effect of materials and processes is on SR and LER and their relation. As soon as the process steps and the material properties have been taken into account and understood, the simulator can easily be extended to take into account the aerial image effects on LER. We will address this problem in the future. Molecular simulations provide one method for the estimation of the microscopic structural changes which occur during the lithographic process.[9,11] A detailed description of the lithographic procedure including reaction propagation, acid diffusion, cage effects, free volume effects, and developer selectivity can be included in such a model. In the present model, an extension of our work[9,11] by inclusion of a developer module for a negative-tone CAR, and a SR and LER estimator are employed. Our present model is applied only for solution developed resists. However, plasma development simulation is in our plans. Our simulations will be checked against experimental data from a negative CAR of known chemistry developed in our laboratory. It is an extremely sensitive (1 $\mu C/cm^2$) high-resolution epoxy containing novolac (EPR),[12] which is however solvent developed. An aqueous-base developed version of this resist is now being evaluated in our laboratory as a fast e-beam resist.[13] The value of our simulation package is not limited to one particular resist, namely EPR. In collaboration with a resist manufacturer, other resist materials can be simulated, provided the details of the resist composition and chemistry are given. The simulation work is described in Sec. III.

II. EXPERIMENTAL STUDY FOR THE SR AND LER OF SILOXANE POLYMERS

For the study of SR and LER of bilayer resists we have used as model materials the siloxane resists, which could be useful for both e-beam and 157 nm lithography, provided they are copolymerized with polymers capable of aqueous base development. In particular a commercial material PDMS (by Aldrich) with a broad molecular weight (MW) distribution ($M_w/M_n=2$), and a material synthesized at the polymer synthesis laboratory of the University of Athens having a very narrow MW distribution ($M_w/M_n=1.01$) were used. The average M_w was the same for both polymers, but obviously M_n is smaller for the Aldrich material. The materials were used as bilayer resists on top of hard-baked novolac AZ5214 resist by Clariant coated on silicon wafers at a thickness of 500–1000 nm. After an initial bake at 90 °C for 90 s, the resist was baked at 200 °C for 15 min. The final bottom resist thickness after the hard bake was 400–800 nm. Subsequently 100 nm thick siloxane films were spin coated on the bottom layer. The resist was exposed with a 50 keV e-beam, solution developed in methylisobutylketone (MIBK), and developed in an oxygen plasma at 10 mTorr pressure in a reactive ion etcher. Two conditions were tried: plasma development without and with a breakthrough step (BTS) (20% SF_6+20% CHF_3+60% O_2 for 6% of the total development time). In both cases, lines were observed by SEM, and pads by AFM. Measurements from two AFM instruments are reported: a Nanoscope III model 423h3 from Digital Instruments, and a Topometrix TMX 2000 system.

Figure 2 shows the results without (top) and with (bottom) BTS for the commercial material (Aldrich). Similar results were obtained with the synthesized material. Without BTS, the high LER and SR are due to the incomplete development of the top layer for this bilayer system. Apparently some residues remain after solution development which, given the high Si content of the siloxane, caused a roughening of the surface in the subsequent plasma development step in the oxygen plasma. The SR is observed as LER at the edges of patterns since the residues at the edges of the lines will cause LER. At high doses the LER is reduced, however SR increases due to the high extent of crosslinking of the overexposed siloxane film with unequal lines and spaces (L/S). This is confirmed by AFM observations and shows that LER and SR may not behave similarly. With a BTS, the LER is now greatly reduced to almost zero. Surface roughness is again high at high doses, due to strong crosslinking.

Figure 3 shows the AFM images of the plasma developed siloxane surfaces (with a BTS) as a function of dose for the commercial material. Similar results were obtained with the synthesized material. The smallest dose is the lithographic useful dose. As the dose increases, a very large increase of the SR is shown and the texture of the surface becomes like a rough ''spaghetti'' or better a honeycomb.

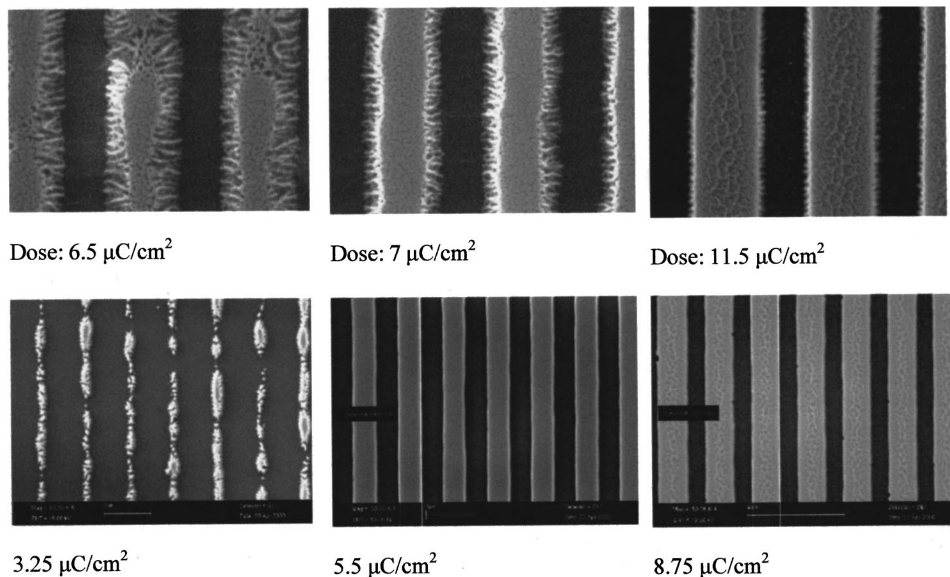

FIG. 2. (Top) 100 nm thick poly (dimethyl siloxane) (Aldrich), was e-beam exposed, solution developed in MIBK, and plasma (O_2– 10 mT– 400 W) developed without a breakthrough step for the 800 nm thick bottom layer. Shown are 0.5 μm L/S. Notice the high LER due to residue and rough edges after MIBK development. Notice also the high SR and the smaller LER at higher doses, which shows that SR and LER do not behave similarly. (Bottom) 100 nm thick poly (dimethyl siloxane) (Aldrich) was e-beam exposed, solution developed in MIBK and plasma (O_2– 10 mT– 400 W) developed after a breakthrough step (20% SF_6+ 20% CHF_3+ 60% O_2 for 6% of the total development time) for the 400 nm thick bottom layer. Shown are 0.5 μm L/S. Notice the much smaller LER of this process. Also notice again the high SR at high doses, where LER is almost absent, but the lines are overexposed.

In Fig. 4 the SR after 1 min oxygen plasma development without and with a BTS step is shown as a function of dose for the synthesized material (the commercial material shows an analogous behavior). In addition to SR data, the contrast curve is displayed without BTS (BTS slightly increases the contrast value, but the contrast curve is not shown to avoid cluttering in Fig. 4). AFM measurements show a minimum of SR at useful doses, and a high SR at high doses. Below approximately 1.5 μC/cm^2, the siloxane film is too thin and breaks down during pattern transfer. Thus, SR increases at low doses, while grass forms. To avoid damaging the AFM tip, we did not measure SR after full development, but only after partial development, i.e., 1 min etching instead of 4 min needed for the end point. The graph shows the large reduction of SR at low doses due to the BTS step, and helps explain the relation between SR and LER and the role of BTS, as follows: Assuming an ideal square-wave exposure profile, the SR on the lines is close to the minimum, while the SR for the spaces is high without a BTS. Thus, as one crosses from the lines to the spaces, SR increases, i.e., LER is present. On the contrary, after BTS the SR in the spaces is very small, and the transition from lines to spaces is smooth, i.e., low LER is observed.

From the literature results,[3,4] a rather universal characteristic of the SR versus dose curve has been observed: SR goes through a maximum as one crosses from very small to useful doses. In plasma developed systems, the SR maximum could actually be ''infinite'' i.e., of the same order as the thickness of the underlayer, and is not measurable by AFM (very high grass). In solution developed systems, such large maxima have been observed in the literature only when partial development was used, because the isotropic solution development process cannot maintain the tall grass as in the case of anisotropic plasma processes.

III. SIMULATION OF SR AND LER

Our SR and LER work includes detailed simulation of SR and LER formation. For the moment, the simulation is applicable only for solution developed negative-tone resists, and has been compared with experimental data for a CAR epoxy novolac resist EPR developed in our Institute.[12,13] Due to the lack of space, we will attempt only a short description of our simulation work.

In order to construct a molecular model of a complex CAR resist system, a three dimensional square lattice is considered. The lattice size is equal to the mean radius of the spherical volume occupied by a monomer. Polymer chains and initiator molecules are placed randomly on that lattice under the following restrictions: (a) the chains are self-avoiding and populate the lattice to the same density as the actual material, (b) the polymerization length has a uniform distribution, and (c) each lattice site can be occupied by no more than one monomer and one initiator molecule. The lattice is filled with the polymer chains by a random walk process, and the photoacid generator (PAG) is randomly distributed in the lattice according to its percent content in the actual material.[11]

The radiation-induced effects are simulated through the use of an initiation probability attributed to each of the PAG molecules. The energy exposure profile can be given by an optical lithography simulator or an electron beam lithography simulator. However, at this stage an ideal square-wave energy profile was used in order to examine the effect of

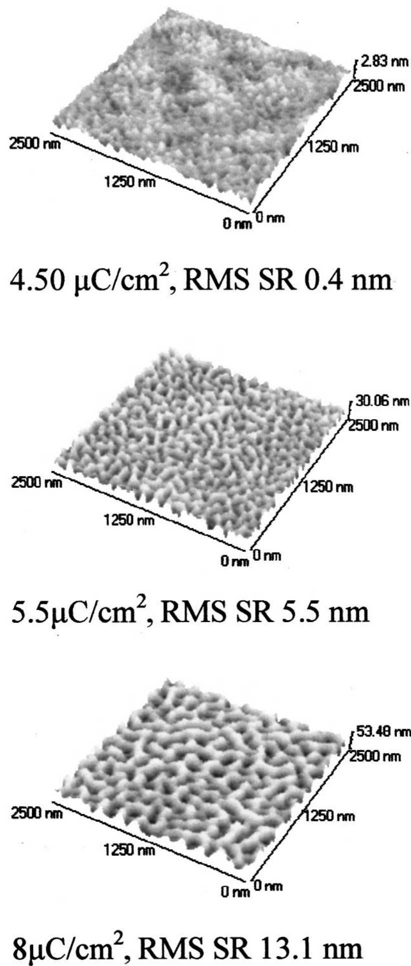

FIG. 3. AFM image of 2500 nm pads. Poly(dimethyl siloxane) (PDMS) (Aldrich) was e-beam exposed, solution developed in MIBK, and plasma (O_2–10 mT–400 W) developed with breakthrough step (20% SF_6 + 20% CHF_3 + 60% O_2 for 6% of the total development time) for the 400 nm thick bottom layer. The first surface at the smallest useful dose is flat and the top silicon containing resist has successfully protected the lower layer. As the dose increases the top layer becomes more and more crosslinked, resulting in high SR.

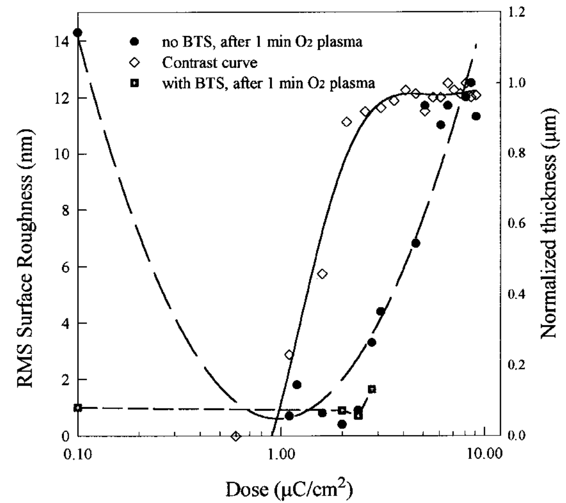

FIG. 4. Contrast curve (empty diamonds) and SR after 1 min partial (25%) plasma development with BTS (filled squares) and without BTS (filled circles) as a function of dose for the synthesized PDMS material. SR has a minimum at useful doses, and is large at high doses. At low doses SR is high without a BTS, but is greatly reduced with a BTS step.

materials and processes on SR and LER independently of the latent image. The energy stored in each cell of the lattice induces acid generation and subsequent reactions. By isolating the outer surface of crosslinks, it is possible to estimate SR or LER before the development process.

The code is not necessarily limited to crosslinking systems and no special change is needed for the consideration of systems based on protection/deprotection chemistry. In that case, the clusters would be interpreted as regions in the material where solubility change has occurred due to exposure.

A detailed model of the development process was also formulated for negative-tone CARs. Developer molecules are inserted in parallel, initially placed along the resist top surface, and move step-by-step in all possible directions in the lattice. Movement is prevented at sites occupied by monomers or crosslinked monomers. The dissolution process is terminated when the whole range of permitted steps per developer molecule has been completed (i.e., the specified development time has elapsed). Partial or full development can be simulated. While the development penetration is in process, the polymer clusters that are surrounded by developer molecules are removed and the final surface line pattern is determined by the developer profile. By isolating the outer surface of the developed profile, it is possible to estimate SR or LER of the resulting structures by calculating rms roughness and fractal dimension. All models are integrated to the same graphical platform and run on a PC.

Figure 5 shows a typical simulation result for a series of L/S. Figure 5(a) shows the coordinates of the crosslinks formed after exposure and postexposure bake. It is clear how a first indication of SR and LER can be obtained from the outer coordinates of the structure. Figure 5(b) shows the coordinates after the development process. The developer has removed some clusters leaving behind the final true structure. Its outer coordinates are used to calculate SR and LER.

Finally Fig. 6 shows our first SR and LER simulations as a function of dose and their comparison with SR experimental data of EPR. The contrast curve of EPR is also shown for reference. The calibration of the dose for our model is done by fitting the simulated contrast curve to the experimental contrast curve of EPR, and by obtaining the relation between dose and initiation probability.[11] Notice that the simulated SR and LER have very similar values and show a maximum at small doses. Roughness then drops very fast to below 3 nm. The trends and values of the simulation results compare well with the SR measured on EPR pads. This successful prediction of the experimental data is indeed very encouraging.

IV. DISCUSSION OF THE RESULTS

A first comparison between the plasma and solution developed resists examined in this article shows that SR can have similar values at the useful doses (see Figs 4 and 6). In

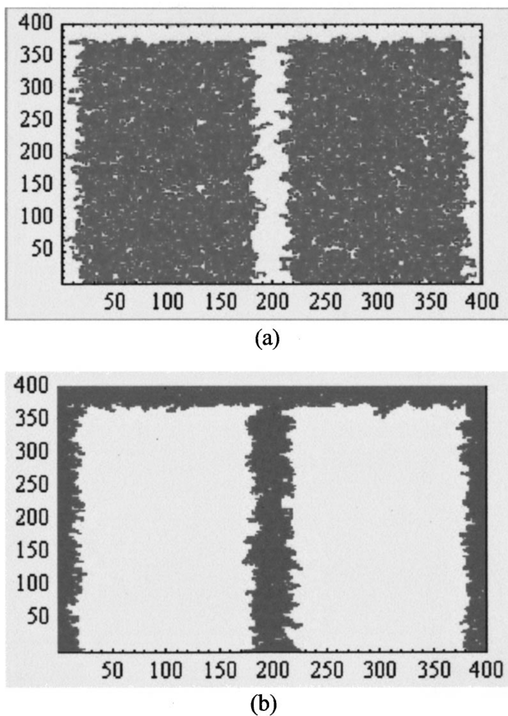

FIG. 5. Graphical representation of the simulation results. A series of lines and spaces is shown: (a) after exposure and postexposure bake. The coordinates of crosslinks are shown and the latent ''roughness'' created by them. (b) After development. The coordinates of remaining crosslinks, i.e., resist profile are shown, and the resulting SR and LER.

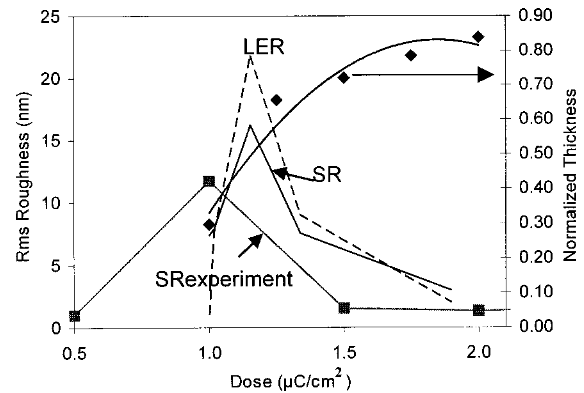

FIG. 6. Contrast curve and roughness versus dose: Symbols stand for SR experimental results of EPR resist containing 1% PAG, which was e-beam exposed, baked at 110 °C, and solution developed in PGMEA; (continuous curve) simulated SR for the same resist; (dashed curve) simulated LER. The left reference point represents measurements of an unexposed surface before development. Simulations refer to a single line of 500 nm wide × 700 nm high.

addition, LER values of the plasma developed resist can be low provided the appropriate BTS step is done. For both resist types, a maximum in the SR versus dose curve results at small doses corresponding to small remaining thickness.

The existence of a maximum in the SR versus dose curve can explain the relation between SR and LER for a real (not square wave) latent image: As one moves from the line to the space (in a lithographic structure of a negative photoresist) one also moves from high to small doses on the SR curve (see Fig. 6). If the latent image were ideal (square wave), the LER would be the same as the corresponding SR at the same dose. However, since the latent image is usually far from ideal, the LER could be climbing up to the maximum of the SR curve. Thus, the further the maximum in roughness is from the gel dose, the less LER will be present in the system.

V. CONCLUSIONS

A framework for the study of SR and LER has been presented. Experimental results from siloxane resists show that such systems have the potential of very low surface roughness, provided the process conditions have been selected accordingly.

A description of our SR and LER simulation was given. It is possible to simulate the change of roughness with dose, development time, acid diffusion length, PAG concentration, and polymer structure. It is also possible to estimate the rms roughness and the fractal dimension of the surface. For the future, we expect to extend the models so as to incorporate the development of positive tone resists and the plasma development of bilayer or silylated resists.

ACKNOWLEDGMENTS

The financial support of ESPRIT Project No. 33562 ''RESIST 193-157'' and Greek Project No. PENED 99ED56 is gratefully acknowledged. The authors also thank Professor Nickolaos Hadjichristidis, Dr. Hermis Iatrou, and Vasilios Bellas of the University of Athens for the synthesis of narrow MW distribution siloxane materials. They also thank Dimitrios Kitsanelis for AFM measurements.

[1]D. He and F. Cerrina, J. Vac. Sci. Technol. B **16**, 3748 (1998).
[2]L. W. Flanagin, V. K. Singh, and C. G. Wilson, J. Vac. Sci. Technol. B **17**, 1371 (1999).
[3]E. W. Scheckler, S. Shukuri, and E. Takeda, Jpn. J. Appl. Phys., Part 1 **32**, 327 (1993).
[4]T. Yoshimura, H. Shiraishi, J. Yamamoto, and S. Okazaki, Appl. Phys. Lett. **63**, 764 (1993).
[5]T. Yoshimura, H. Shiraishi, J. Yamamoto, and S. Okazaki, Jpn. J. Appl. Phys., Part 1 **32**, 6065 (1993).
[6]W. Chen and H. Ahmed, Appl. Phys. Lett. **62**, 1499 (1993).
[7]L. Lai and E. A. Irene, J. Vac. Sci. Technol. B **17**, 33 (1999).
[8]T. Yamaguchi, H. Namatsu, M. Negase, K. Kurihara, and Y. Kawai, Proc. SPIE **3678**, 617 (1999).
[9]G. P. Patsis, N. Glezos, I. Raptis, and E. S. Valamontes, J. Vac. Sci. Technol. B **17**, 3367 (1999).
[10]J. Shaw, M. Hatzakis, E. Babich, and J. Paraszczak, Solid State Technol. **June**, 83 (1987).
[11]G. P. Patsis and N. Glezos, Microelectron. Eng. **46**, 359 (1999).
[12]P. Argitis, I. Raptis, C. J. Aidinis, N. Glezos, M. Bacciochi, J. Everett, and M. Hatzakis, J. Vac. Sci. Technol. B **13**, 3030 (1995).
[13]N. Glezos *et al.*, J. Vac. Sci. Technol. B, these proceedings.